
Figures and figure supplements

Architecture of the ring formed by the tubulin homologue FtsZ in bacterial cell division

Piotr Szwedziak, et al.

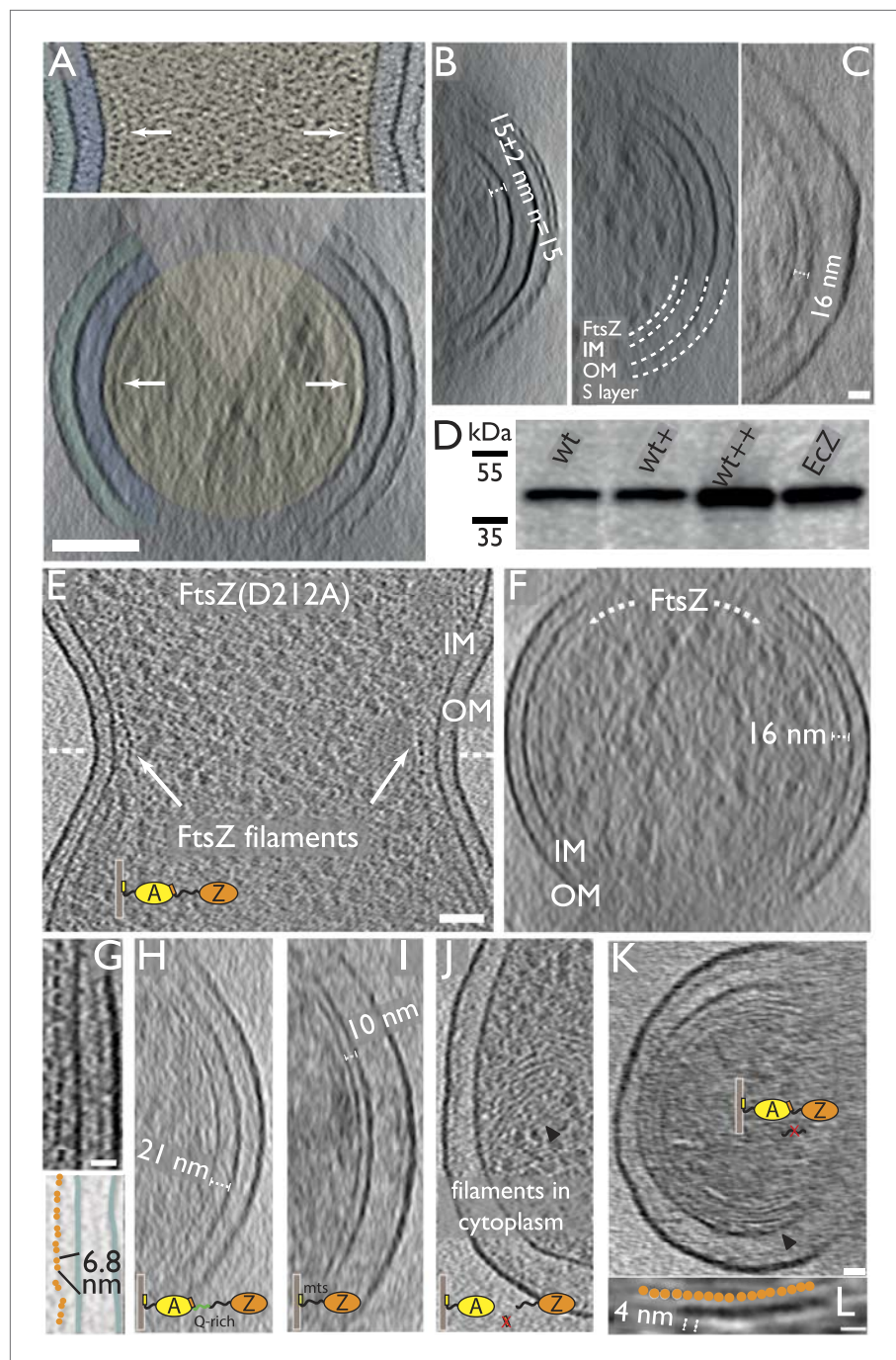


Figure 1. FtsZ forms bands of filaments completely encircling *C. crescentus* and *E. coli* division sites, as visualised by electron cryotomography. (A) *C. crescentus* NA1000/CB15N division site with filaments near the inner membrane IM (top panel, black dots highlighted by arrow, see also **Video 1**). Bottom panel shows the same cell rotated 90° around the short axis of the cell. The Z ring (arrow) is continuous and only invisible where there is no image because of the missing wedge (shaded triangle) (see **Figure 1—figure supplement 1** for more details on the missing wedge problem). The cytoplasm (beige), periplasm (blue), and space between the OM and S layer (cyan) have been coloured for clarity. (B) More examples of continuous FtsZ rings found in *C. crescentus* cells. The filaments were on average 15 nm from the inner membrane. (C) Electron cryotomographic slice of the constriction site of a B/r H266 *E. coli* cell visualised perpendicular to the longitudinal axis, showing very similar FtsZ filaments when compared to *C. crescentus* (**Figure 1A,B**) and FtsZ(D212A) expressing *E. coli* cells (**Figure 1F**) and having roughly the same distance (16 nm) to the IM. **Video 2** demonstrates the likely helical nature of the arrangement of **Figure 1**. Continued on next page

Figure 1. Continued

the FtsZ filaments (see also **Figure 1—figure supplement 2**). **(D)** Western blot showing total FtsZ levels in cells used in **(E–G)** are about 2.5× that of wild-type cells. (+) refers to un-induced, (++) was induced by 0.02% arabinose. EcZ is purified *E. coli* FtsZ protein. **(E–G)** 10-nm thick electron cryotomographic slices of *E. coli* cells expressing FtsZ(D212A) protein in a wild-type B/r H266 background. See also **Figure 1—figure supplement 3**. **(E)** *E. coli* division site showing the cross-section of FtsZ filaments (single row of black dots) at the constriction site. See **Video 3**. **(F)** Visualisation of the same cell along the longitudinal axis shows that FtsZ filaments are located ~16 nm from the inner membrane (IM). **(G)** Closer examination of the constriction site of another cell with higher expression level reveals FtsZ filaments form pairs, appearing as doublets of dark dots (upper) and orange spheres in the schematic illustration, on average 6.8 nm apart within the doublets (lower). **(H–K)** 10-nm thick electron cryotomographic slices of *E. coli* cells expressing engineered protein constructs based on FtsZ(D212A) (see also **Figure 1—figure supplements 3,5** and **Supplementary file 1, Table B**). **(H)** Extending the C-terminal linker of FtsZ by inserting a linker sequence pushes the filaments further away from the IM (distance changed from 16 nm to a somewhat variable 16–21 nm). **(I)** Replacing the C-terminal FtsA-binding sequence of FtsZ with a membrane-targeting sequence (mts) makes FtsZ directly bind to the IM and results in FtsZ filaments closer to IM (distance changed from 16 nm to 10 nm). No cell constrictions were observed with this construct. **(J)** Removing the C-terminal FtsA-binding sequence of FtsZ renders it unable to maintain a fixed distance to the IM and FtsZ filaments that were observed within the cytoplasm. **(K)** Removing the C-terminal flexible linker of FtsZ makes it prone to form multiple layers of filaments that form complete rings or helices. Tomography using this construct works better because it produces small minicells. **(L)** A closer inspection of the area marked with the black arrowhead in G shows beads along the filament as illustrated by the schematic drawing with a repeat distance of 4 nm as expected for FtsZ filaments. IM: inner membrane; OM: outer membrane; WT: wild-type; Q-rich: FtsN-derived flexible linker; mts: membrane-targeting sequence. Scale bars: 100 nm in **(A)** and **(B)**, 50 nm in **(E, F, H, I, J)**, 20 nm in **(C, G, K)**, 10 nm in **(H)**, 20 nm in **(L)**. DOI: [10.7554/eLife.04601.003](https://doi.org/10.7554/eLife.04601.003)

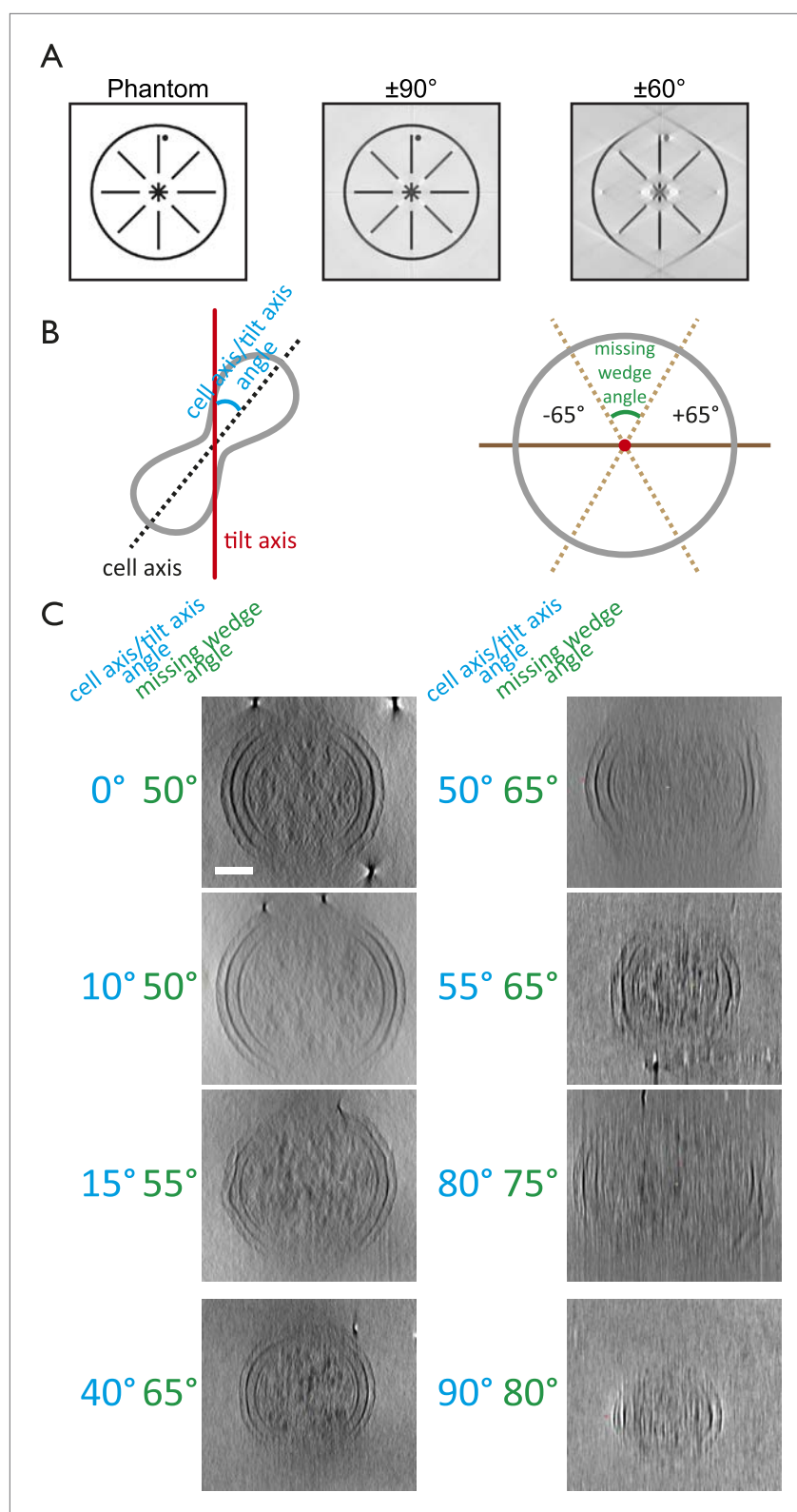


Figure 1—figure supplement 1. The missing wedge problem in cellular electron cryotomography. Since it is impossible to tilt the sample support (EM grids) from -90° to $+90^\circ$ and because the thickness of the ice film increases at high tilt angles, electron tomograms miss significant amounts of data. **(A)** Simulation of the effects of the missing wedge. Modified from [Palmer and Löwe, \(2013\)](#). A phantom image resembling a cell envelope was

Figure 1—figure supplement 1. Continued on next page

Figure 1—figure supplement 1. Continued

reconstructed for a full $\pm 90^\circ$ range and a $\pm 60^\circ$ range, the latter being typical for tilt series acquisition. (B) Schematic drawings explaining the angle (blue) between the tilt axis (red) and the cell axis (black dashed line) and the missing wedge angle (green). The former can be anything between 0 and 90° , whereas the latter can be anything between 0 and 180° . Tilt series for the *C. crescentus* study (Figure 1A–B) were obtained using the $\pm 65^\circ$ range. (C) Examples of the effects of different orientations of cells in the microscope with respect to the tilt axis on the missing wedge. Cells that were aligned with the tilt axis produced the most complete tomograms since the cell thickness stayed constant over the angular range. High tilts of those perpendicular to the tilt axis did not provide any useful information since the effective cell thickness in the electron beam increased. Shown are projections along the long axis of the cell. It is important to note that the angle between the tilt axis and the longitudinal axis of the cell is crucial in order to obtain high quality tilt series, other factors such as cell thickness, ice thickness, and membrane invagination progression also affect the quality of the resulting tomograms significantly. Scale bar: 100 nm.

DOI: [10.7554/eLife.04601.004](https://doi.org/10.7554/eLife.04601.004)

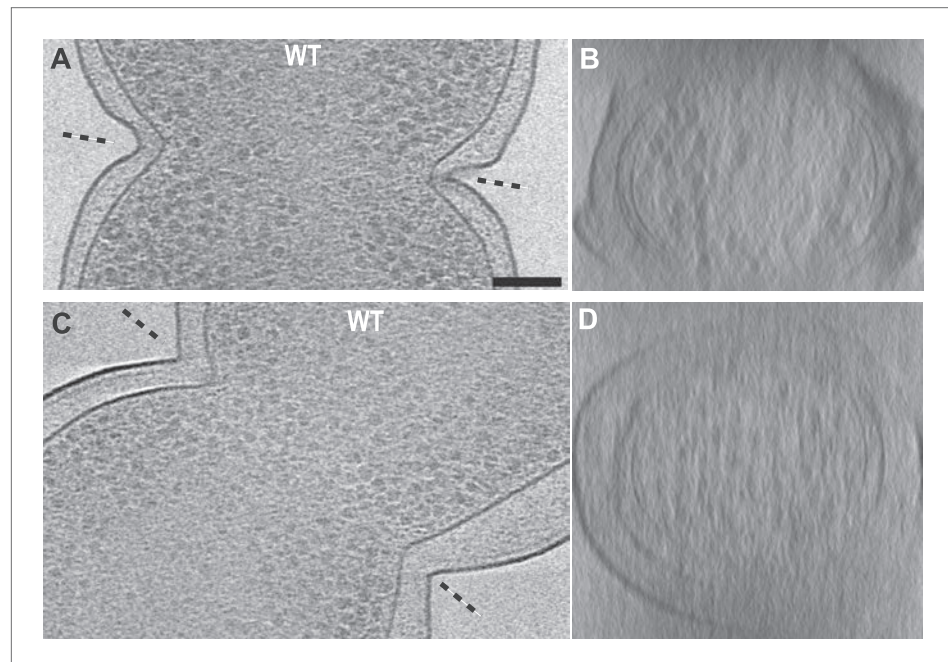


Figure 1—figure supplement 2. Electron cryotomograms of wild-type *E. coli* cells show filaments at the constriction sites. (A, C) 10-nm thick tomographic slices of two cells showing black dots near the constriction sites corresponding to cross-sections of filaments. Filaments are difficult to discern in this viewing direction because of the thick *E. coli* cells (B, D) Filaments are better visualised when viewed perpendicular to the constriction planes showing filaments near the IM. These images, together with Video 2, suggest that FtsZ forms a closed ring with slight helicity near the constriction site.

DOI: [10.7554/eLife.04601.005](https://doi.org/10.7554/eLife.04601.005)

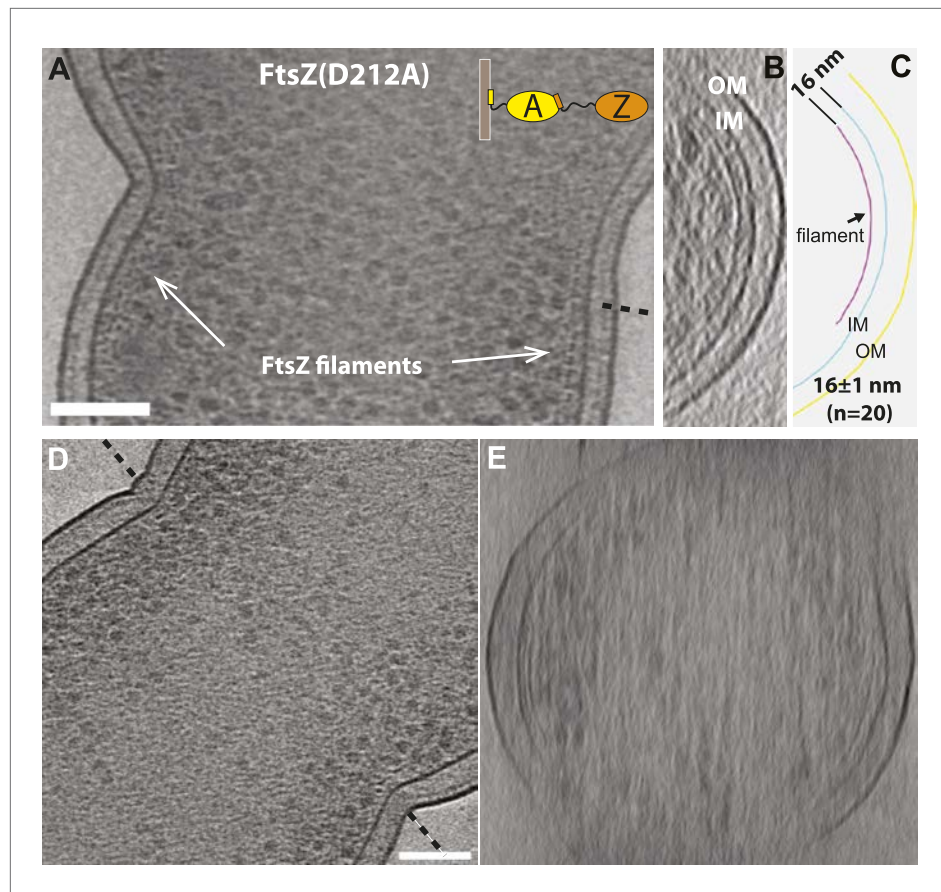


Figure 1—figure supplement 3. FtsZ forms bands of filaments at constriction sites in *E. coli* cells. (A) 10 nm electron cryotomographic slice of a cell expressing more FtsZ(D212A) protein than in **Figure 1E** (corresponds to **Figure 1G**), oriented parallel to the longitudinal axis, showing one layer of dots near the constriction site, corresponding to cross-sections of FtsZ filaments that are 16 nm away from the IM. (B) Electron cryotomographic slice of the cell viewed perpendicular to the dashed line in (A). FtsZ filaments and their relative position to the IM are illustrated with the schematic representation of the tomographic slice in (C). (D–E) 10 nm electron cryotomographic slices of a cell with very low level expression of FtsZ(D212A) protein (un-induced) viewed parallel to the longitudinal axis in (D) and perpendicular to the dashed line in (D), showing similar architecture of FtsZ filaments at the constriction site. Scale bars: 100 nm.

DOI: [10.7554/eLife.04601.006](https://doi.org/10.7554/eLife.04601.006)

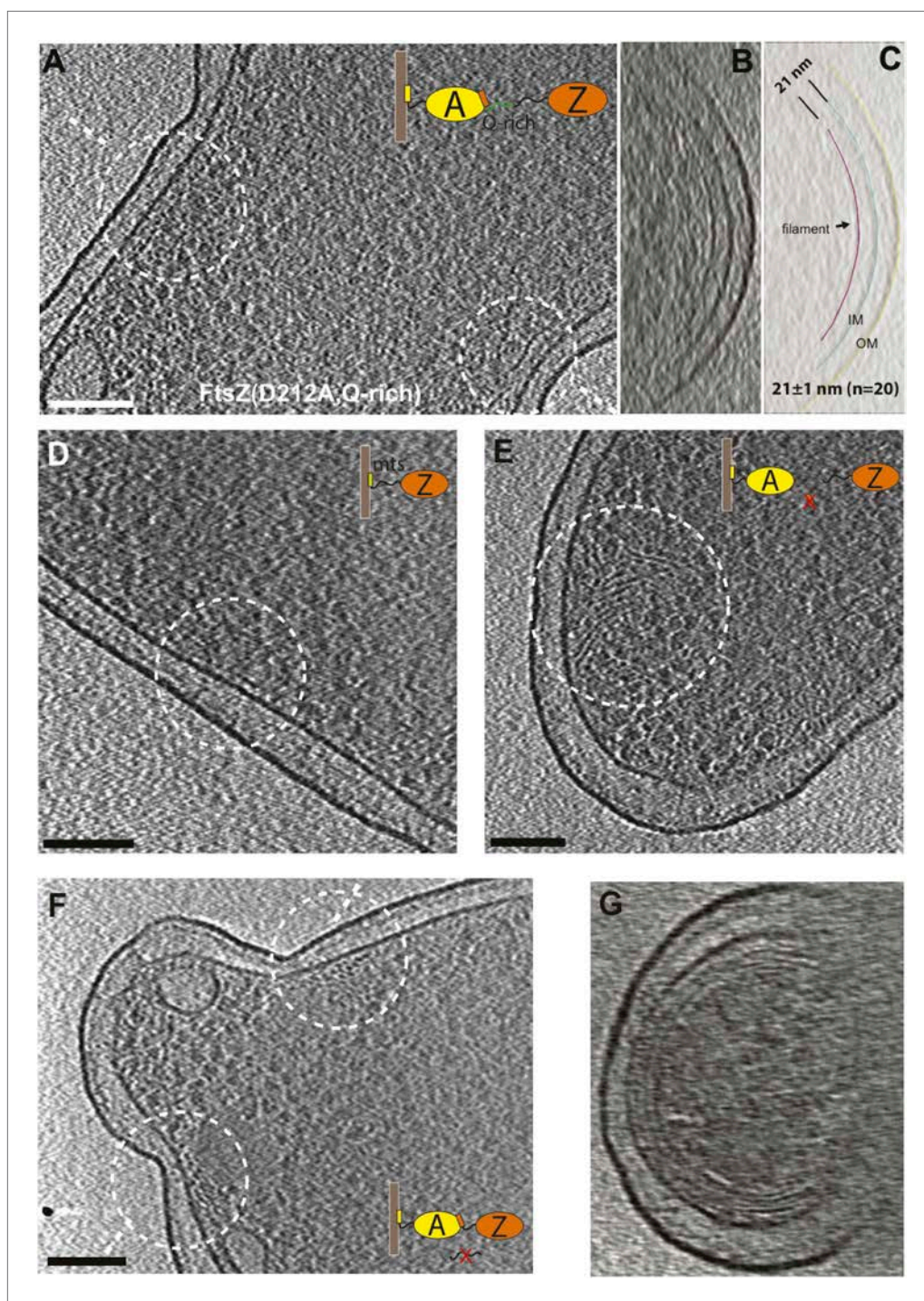


Figure 1—figure supplement 4. Engineered FtsZ proteins form filaments with altered localisation patterns in *E. coli* cells. (A) Extending the C-terminal flexible linker of FtsZ(D212A) makes the protein form filaments further away from the membrane with a distance to IM increased from 16 nm to 21 nm; (B) and (C) are tomographic slices of the cell viewed perpendicular to the dashed lines in (A) and segmentation illustrating the relative positions of FtsZ filaments and the IM; (D) cells expressing a membrane-binding FtsZ construct produced by fusing the *E. coli* MinD membrane-targeting sequence (mts) to the C-terminus of FtsZ produce filaments that are 10 nm away from IM; (E) removing the C-terminal FtsA-binding sequence of FtsZ gives filaments further away from the IM; (F) FtsZ without the C-terminal flexible linker tends to form multiple layers of filaments near the constriction site, and (G) such filaments appear to form complete rings or helices when viewed perpendicular to the plane of cell constriction. Scale bars: 100 nm.

DOI: [10.7554/eLife.04601.007](https://doi.org/10.7554/eLife.04601.007)

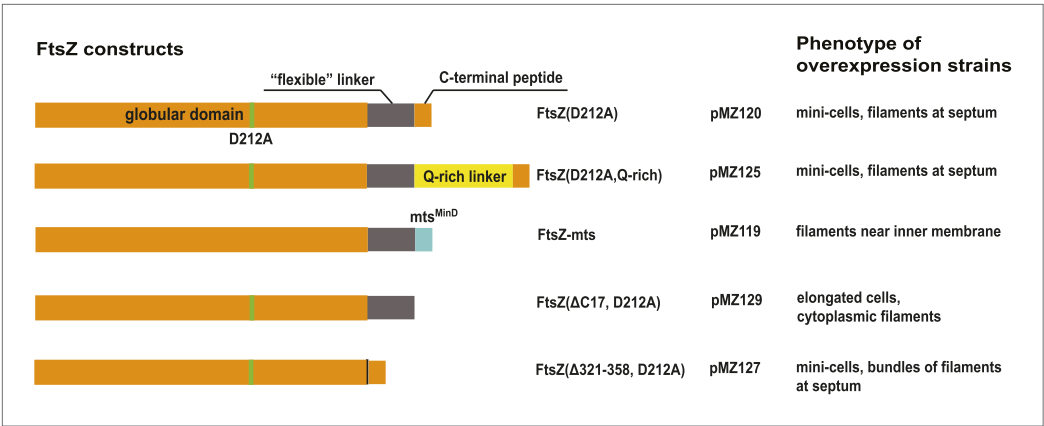


Figure 1—figure supplement 5. Overview of FtsZ constructs used for in vivo tomography. Please also consult *Supplementary file 1A,B*.
DOI: [10.7554/eLife.04601.008](https://doi.org/10.7554/eLife.04601.008)

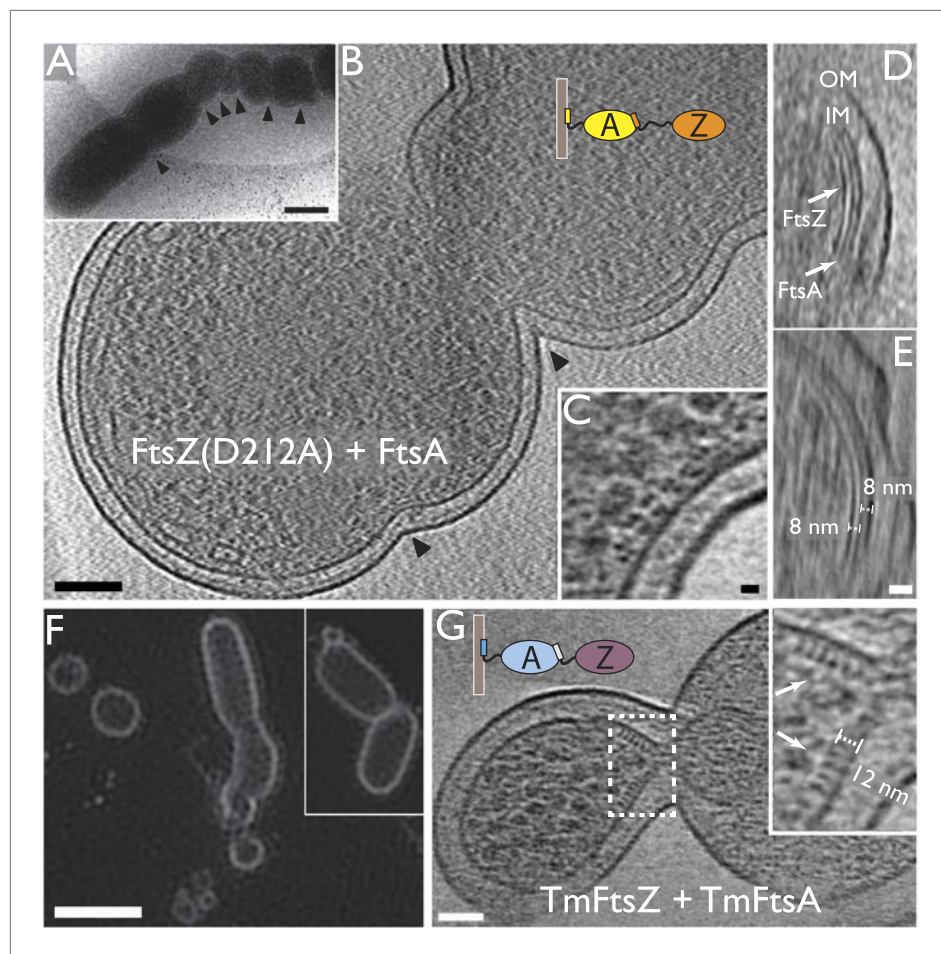


Figure 2. Co-expression of FtsZ and FtsA in *E. coli* cells leads to extra septa. (A) A low-magnification 2D electron cryomicrograph (transmission) showing multiple constriction sites (marked with black arrowheads) along the cell. (B–E) 10-nm thick electron cryotomographic slices of cells co-expressing FtsZ(D212A) and FtsA (bicistronic, 1:1). Two layers of dots are visible at constriction sites in (B) and (C), corresponding to FtsZ filaments and FtsA filaments, respectively, as labelled in the orthogonal view along the long axis of the cell (D). FtsA filaments are almost in the middle between FtsZ filaments and the IM, at a distance of 8 nm from both FtsZ filament and IM as indicated in (E). (F) Structured illumination microscopy images of cells expressing FtsZ(D212A) and FtsA, showing cell division and minicell formation, proving that the extra septa function to completion. (G) 10-nm thick electron cryotomographic slice of an *E. coli* minicell formed from cells expressing *Thermotoga maritima* FtsZ and FtsA proteins, with a deeply constricted area showing cross-sections of FtsZ and FtsA filaments (black dots marked with white arrows). Distance between FtsZ filaments and IM is around 12 nm (inset in G). The view highlights striking similarities to the in vitro reconstruction shown in Figure 3H–J & 5C. IM: inner membrane; OM: outer membrane. Scale bars: 500 nm in (A), 100 nm in (B), 10 nm in (C, and also for inset in G), 20 nm in (E, and also for D), 2 μ m in (F).

DOI: [10.7554/eLife.04601.012](https://doi.org/10.7554/eLife.04601.012)

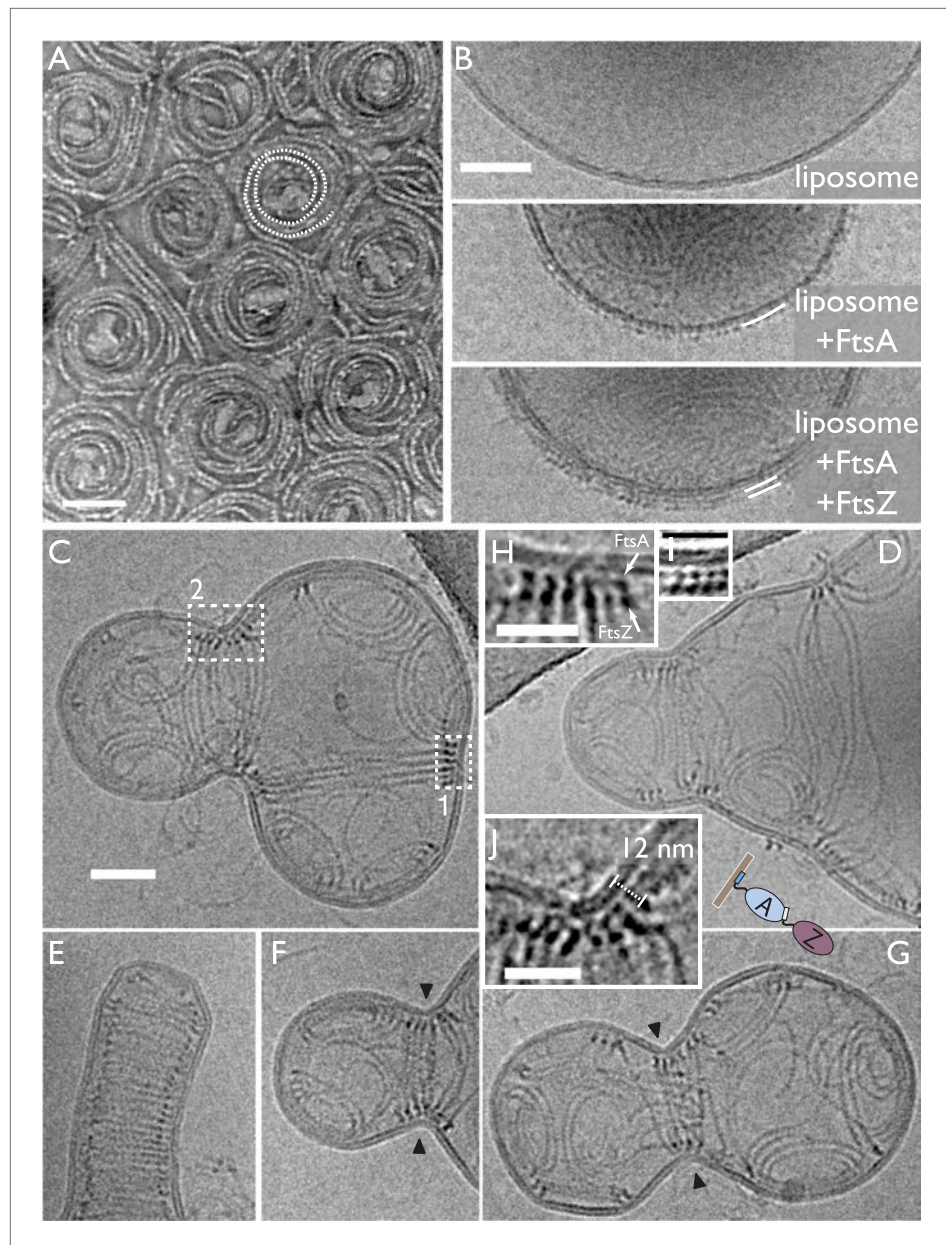


Figure 3. In vitro reconstitution of bacterial cell membrane constriction by the FtsZ ring from purified components. **(A)** *Thermotoga maritima* FtsA (TmFtsA) and *Thermotoga maritima* FtsZ (TmFtsZ) form spirals on a flat lipid monolayer, as indicated by a white dotted line. The filaments tend to appear as double strands (doublets). Negative-stain electron microscopy. **(B)** Transmission electron cryomicroscopy allows resolution of the inner and outer leaflet of undisturbed liposomes (top panel). When TmFtsA is added to the outside, an additional layer of density corresponding to FtsA becomes apparent (middle panel). Recruitment of TmFtsZ by TmFtsA leads to the formation of two layers (bottom panel). Taken together, we conclude that FtsA is sandwiched between the membrane and FtsZ filaments (bottom panel). See also **Figure 3—figure supplement 1** and **Figure 3—figure supplement 2**. **(C–G)** Constriction sites are efficiently formed when TmFtsA and TmFtsZ are encapsulated in liposomes that have sizes comparable to bacterial cells. Five representative liposomes are shown using transmission electron cryomicroscopy (hence are 2D projections of 3D objects). Importantly, constriction sites are only formed where a ring made of the two proteins is present (black arrowheads) and not at other sites where filaments are located. The TmFtsA and TmFtsZ layers are clearly visible (inset **H**, same as boxed area '1' in **C**; inset **J**, same as boxed area '2' in **C** and inset **I**, which is from **Figure 4** electron cryotomography data) and the protein's organisation mirrors that present in *E. coli* cells (compare with **Figure 2C**). The distance of 12 nm between TmFtsZ and the

Figure 3. Continued on next page

Figure 3. Continued

membrane (inset **J**) resembles that found in over-expressing cells (see **Figure 2G** and also **Figure 5C**). (**E**) Intriguingly, liposomes are being constricted (partially) in the absence of added nucleotide. Scale bars: 50 nm in (**A–C**), 25 nm for insets.

DOI: [10.7554/eLife.04601.013](https://doi.org/10.7554/eLife.04601.013)

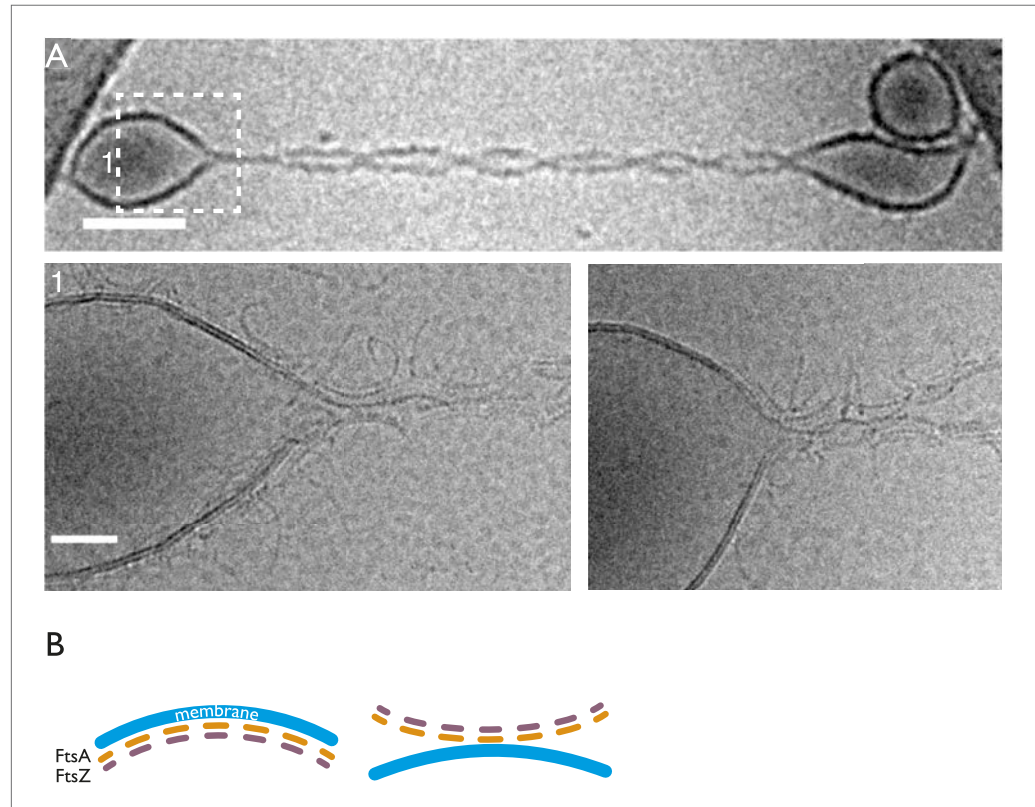


Figure 3—figure supplement 1. TmFtsZ and TmFtsA on the outside of liposomes and in the presence of GMPCPP deform liposomes. (**A**) Low-magnification (upper panel). More detailed snapshots (lower panel) show that the filaments are on the outside; however, they do not form rings but curved structures that are positioned in areas of negative membrane curvature that they probably induce. (**B**) Schematic representation of the curvature produced by co-polymerisation of FtsA and FtsZ, which have differing repeat distances of 5 and 4 nm, respectively. Since FtsA binds to the membrane, this arrangement will lead to negative curvature. Hence, the intrinsic, negative curvature of the FtsA:FtsZ filaments fits the curvature of the membrane on the inside. However, on the outside, the membrane curvature is positive, as is also shown in **Figure 4—figure supplement 1**.

DOI: [10.7554/eLife.04601.014](https://doi.org/10.7554/eLife.04601.014)

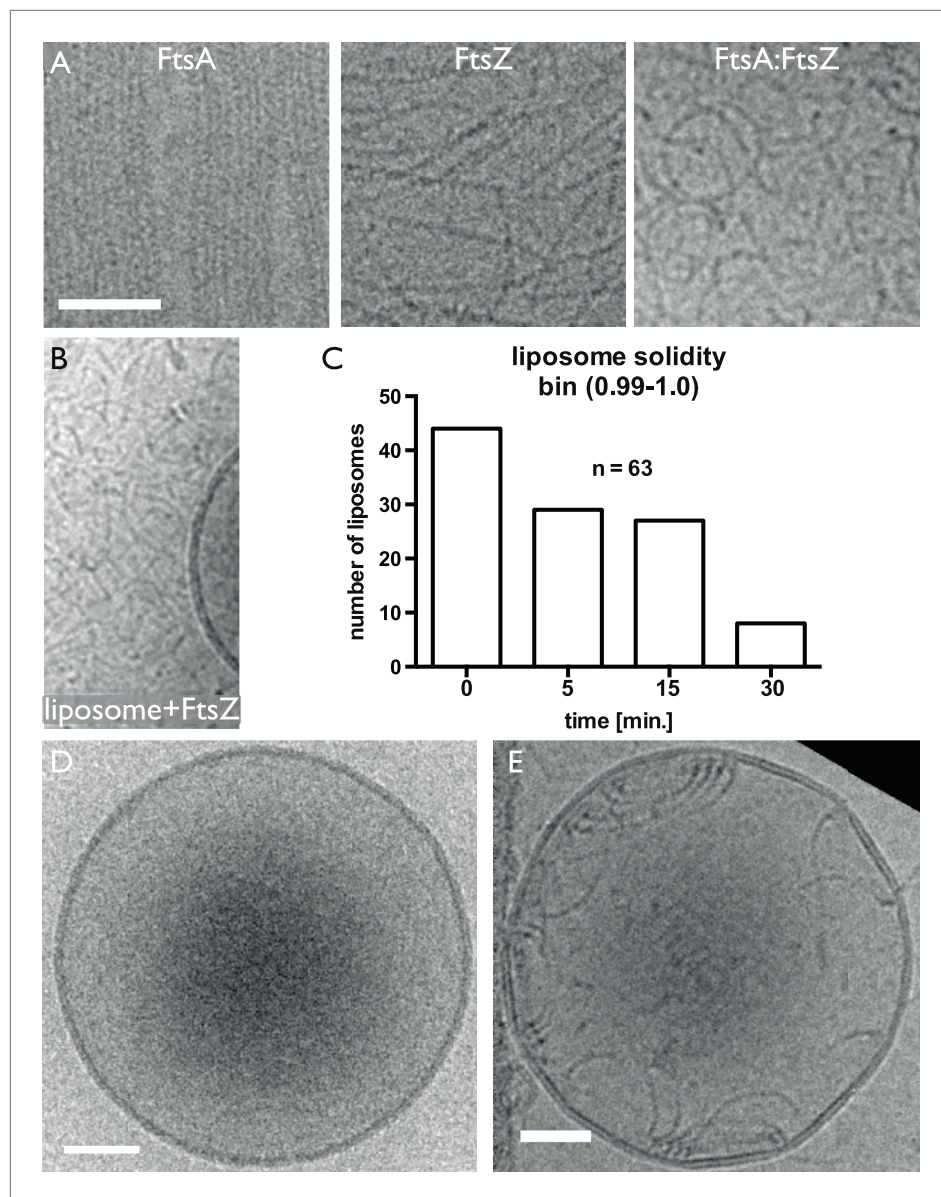


Figure 3—figure supplement 2. Control experiments showing that both TmFtsA and TmFtsZ form straight filaments when polymerised separately. And liposomes deform mostly after dilution. **(A)** When mixed, FtsA and FtsZ form curved filaments (right panel). **(B)** TmFtsZ does not bind to liposomes on its own. Random electron cryomicroscopy images taken immediately after detergent dilution were analysed for liposome deformations. The plot in **(C)** shows the number of liposomes, out of 63, that are perfectly round (as per solidity quantity, defined in (ImageJ)). Clearly, liposomes become more deformed over a 30-min period after dilution. **(D)** Shows a spherical liposome without proteins added and **(E)** at time point 0 min, right after dilution. Scale bars 50 nm.

DOI: [10.7554/eLife.04601.015](https://doi.org/10.7554/eLife.04601.015)

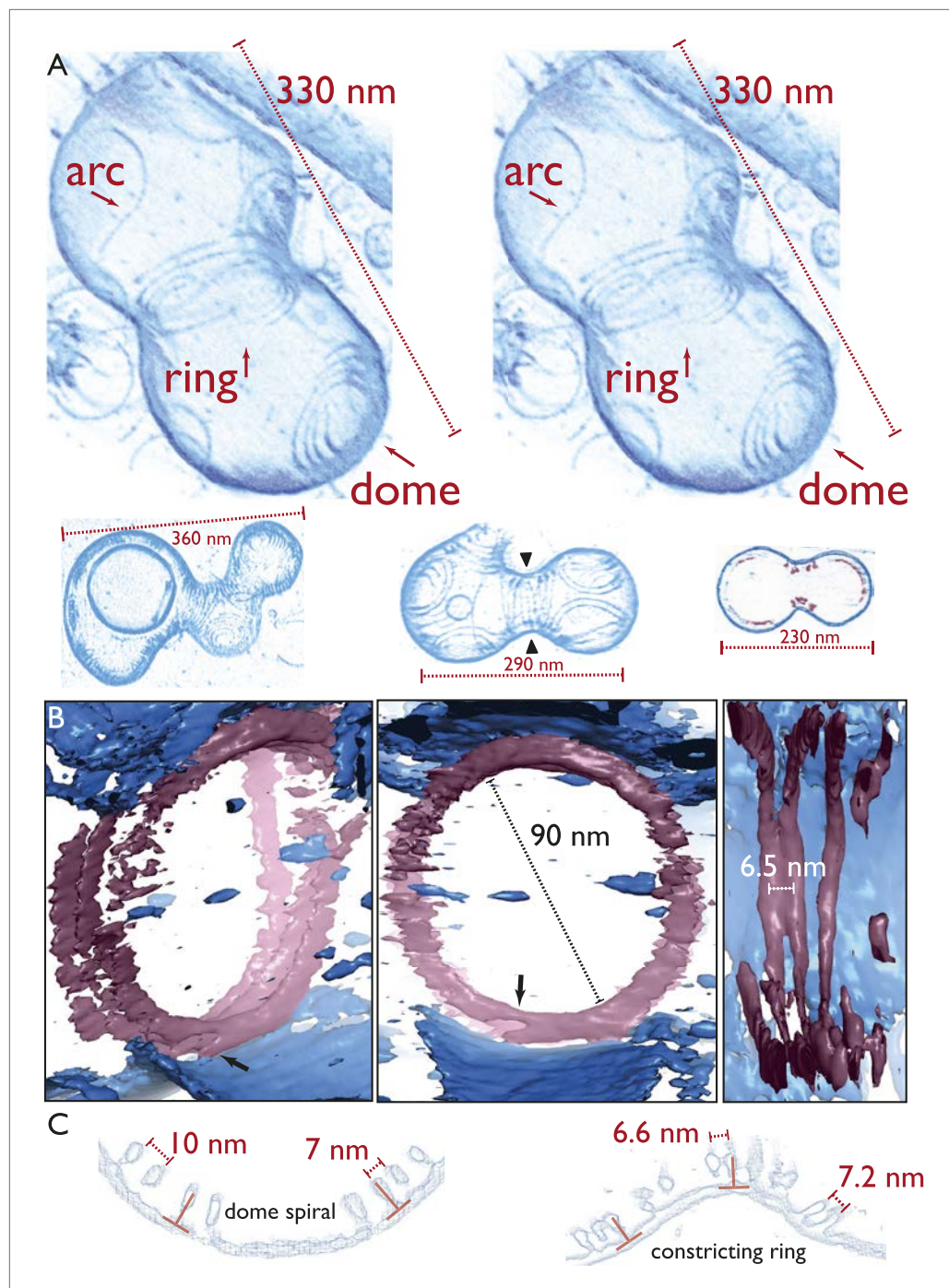


Figure 4. Electron cryotomography of liposomes constricted in vitro by rings of TmFtsA and TmFtsZ. (A) Stereo view of a representative liposome highlighting three different structures made by the enclosed TmFtsA and TmFtsZ proteins. Note that our images derived from tomographic volume data have not been segmented, they are volume representations of the actual 3D tomographic data. Arcs (also on the outside) are filaments made of both FtsA and FtsZ, whose curvature is determined by the mismatch in TmFtsA and TmFtsZ polymers subunit spacing (5 nm vs 4 nm, see also **Figure 3—figure supplement 1** & **Figure 4—figure supplement 2**). Dome-like structures are slightly helical spirals of condensing TmFtsZ filaments attached to the membrane by TmFtsA. Importantly, only complete rings seem capable of constriction force generation. The ring might consist of overlapping filaments (as in the stereo view and **Video 10**) or maybe a continuous helix of double filaments (bottom panel, middle liposome with black arrowheads, see also **Figure 4—figure supplement 1** and **Video 6**). The bottom panel depicts more

Figure 4. Continued on next page

Figure 4. Continued

examples of different liposome shapes and sizes. The cross-section (right) shows the distribution of filaments (red) inside a liposome (membrane in blue) (bottom right). **Video 4** shows a complete 3D volume in grey scale. **Video 5** shows a slice view at high magnification, demonstrating the excellent contrast these specimens generate, making it possible to see individual subunits and complete filament traces. **Videos 6–9** show 3D views of several constricted liposomes. **Figure 4—source data 1** enables 3D viewing of a liposome volume with PyMOL. **(B)** Close-up view of the FtsZ ring (purple) attached to the membrane (blue), here shown as single-threshold surface representations (these are not automatic or manual segmentations). The filaments overlap and interact laterally (left panel). View along the long axis shows that the ring is a perfect closed circle (middle panel). The black arrow points to where TmFtsZ and TmFtsA filaments are fully detached from each other. Individual filaments are resolved (right panel). **Video 10** shows a 3D walk-through the liposome, highlighting most features on the way. **(C)** Comparison of filament arrangements and geometries within the dome-like structures (left panel) and ring-like structures (right panel). Cross-sections demonstrate that in both cases, the TmFtsAZ filaments are positioned close to perpendicular with respect to the membrane (red symbols). However, the constriction force is generated only in the rings (see **Figure 5D** for explanation).

DOI: [10.7554/eLife.04601.016](https://doi.org/10.7554/eLife.04601.016)

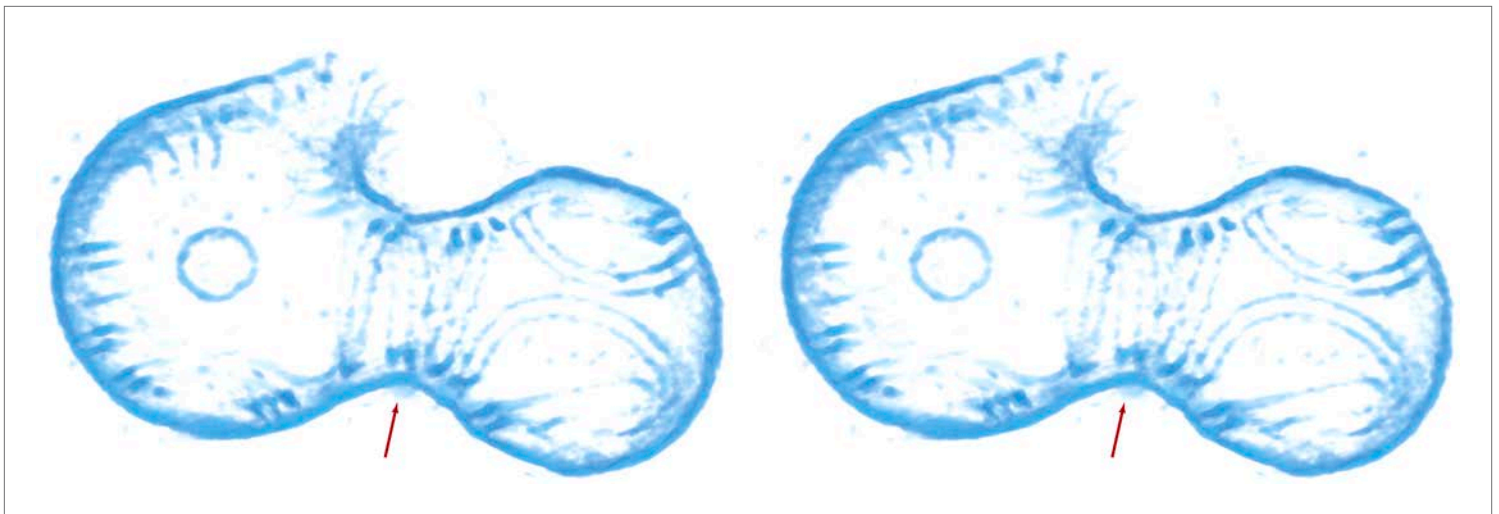


Figure 4—figure supplement 1. Constrictions occur only at the site of filament ring formation. A stereo view of the liposome marked with the black arrowheads in **Figure 4A** (bottom middle panel). A single helix made of filament doublets is marked with red arrow. **Video 6** shows its architecture in more detail and in 3D.

DOI: [10.7554/eLife.04601.018](https://doi.org/10.7554/eLife.04601.018)

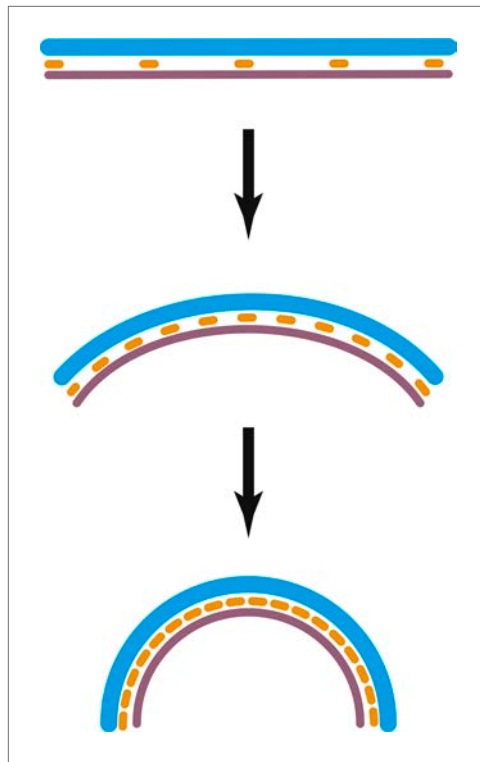


Figure 4—figure supplement 2. A mechanism explaining variable intrinsic FtsA:FtsZ filament curvature. At some stages of constriction, the ratio of FtsZ to FtsA in the ring may be higher than one. Normally, there is around five times more FtsZ in cells than FtsA, therefore only a few FtsA molecules may be sandwiched in between the IM and FtsZ filaments (which form more easily than FtsA filaments), upper panel. As curvature increases, the mismatch of the FtsA (orange) and FtsZ (grey) repeats (5 vs 4 nm, respectively) makes it possible to add more FtsA since the double filament ‘wants’ to bend. Full occupancy of both FtsA and FtsZ in the double filament leads to a curvature of about 60 nm. This mechanism could be another source of energy for constriction in addition to or alternative to the condensation energy gained from filament overlap (mechanism **B**) in the discussion.

DOI: [10.7554/eLife.04601.019](https://doi.org/10.7554/eLife.04601.019)

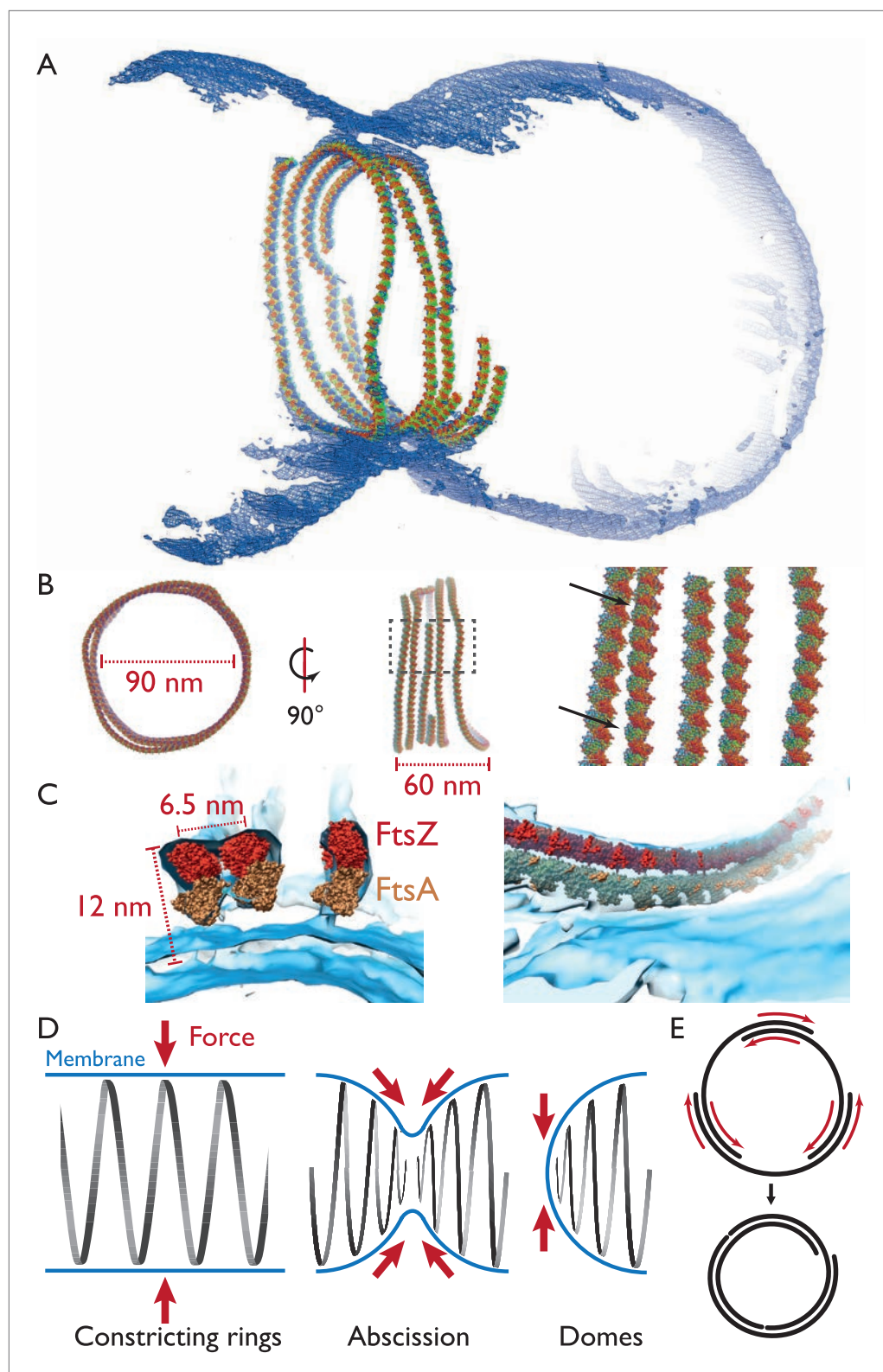


Figure 5. Visualising the FtsZ ring at the molecular level. (A) A semi-atomic model of the FtsZ ring constricting a liposome. 294 monomers of *S. aureus* FtsZ have been roughly positioned using a spline-fitting approach (PDB 3VO8 (Matsui et al., 2012)). This uses the same tomography data as Figure 4A. (B) The ring is 90 nm in diameter (left) and 60-nm thick (middle). It consists of at least four individual filaments (right, atoms shown as spheres) with Figure 5. Continued on next page

Figure 5. Continued

varying lateral interfilament distances (right, atoms shown as spheres, black arrows). (C) FtsZ filaments are single protofilaments, but they tend to pair in doublets. A precision manual fit of the TmFtsA polymer crystal structure (PDB 4A2B) (Szwedziak et al., 2012) in addition to 3VO8 FtsZ polymer crystal structure was performed in a region of very good density. The fit is excellent and dimensions and distances match well with CcFtsZ, EcFtsZ, and TmFtsAZ in vivo situations (Figure 1A,E, 2E,G). (D) Left: in the ring-like structures (black), force (red arrows) is perpendicular to the membrane (blue), leading to constriction. Middle: during constriction, the ring develops into two helical spirals, leading to forces pushing membrane inwards, and this might explain how abscission is accomplished since membranes will presumably not fuse while the protein filaments are in between (see Figure 4A bottom right and Video 9 for an example of this in liposomes). Right: the domes we observed do not deform liposomes because the force generated is almost perfectly tangential to the membrane. (E) Constriction force generation and filament sliding. In the discussion, three different energy sources for constriction are listed: maximising filament overlap, repeat mismatch within FtsA–FtsZ copolymers (Figure 4—figure supplement 2) and filament shortening and turnover due to nucleotide hydrolysis by FtsAZ. While it is currently not obvious which of these or if a combination of the three mechanisms drives constriction, it seems clear to us that constriction, at least in the liposome reconstitution experiments, requires filaments to slide past each other as is depicted in two dimensions. Since also unmodified wild-type cells (Figure 1) show closed continuous rings at division sites, we would assume the same holds true in vivo. Filament sliding can also explain the spirals on lipid monolayers (Figure 3A) and spirals in the dome-like structures with liposomes (Figure 4A). The schematic drawn is a simplification into two dimensions, of course, in vivo and in vitro FtsZ filaments overlap in the third dimension, forming single-layered bands since each filament is anchored to the membrane.

DOI: [10.7554/eLife.04601.027](https://doi.org/10.7554/eLife.04601.027)